Journal of Inclusion Phenomena 3, 461–469. 0167–7861/85.15.

Mechanistic Model of Disproportionation of Nitrogen Monoxide on CaHY-type Zeolite

Y. KANNO★
Government Industrial Research Institute, Nagoya, Hirate-cho, Kita-ku, Nagoya 462, Japan

Y. MATSUI★★ and H. IMAI
Research Laboratory of Engineering Materials, Tokyo Institute of Technology, Nagatsuta-cho, Midori-ku, Yokohama 227, Japan

(Received: 21 February 1985)

Abstract. Infrared spectra produced by adsorbing, by evacuating and by readsorbing NO on CaHY-type zeolite were examined. The absorption peaks were identified by comparing the spectra produced by adsorbing and by evacuating N_2O and NO_2. Based upon the experimental evidence, an eight-step mechanism was proposed for the behavior of NO on CaHY-type zeolite. A mechanistic model of the disproportionation reaction of NO was deduced from the variation of the spectra with time.

Key words: Nitrogen monoxide, IR spectroscopy, disproportionation reaction, CaHY-type zeolite.

1. Introduction

Addison and Barrer first reported that the disproportionation reaction of NO occurs on chabazite, faujasite, and A-type zeolites at 0 °C or lower temperatures [1]. From the material balance and the specific gravity measurement of product gas, they proposed the following disproportionation scheme: $4\,NO \rightarrow N_2O + N_2O_3$.

In an infrared study of adsorbed NO on A- and X-type zeolites, Alekseyev *et al.* were confident of the existence of the chemisorbed N_2O species, and the peaks at 1940 and 2100 cm^{-1} were assigned to covalently bonded NO and ionically bonded NO^+ respectively [2]. Later, Chao and Lunsford also studied the reaction on NaY- and CaY-type zeolites, and deduced a mechanism for the disproportionation reaction of NO [3].

Based on the pulse-reaction technique, we have investigated recently the catalytic activity of Y-type zeolites exchanged with various metal ions towards the disproportionation of NO [4]. From the amount of adsorption of CO it was deduced that the active sites for the disproportionation reaction of NO are metal ions located on Site II of the faujasite structure [5,6]. Studies of Y-type zeolites with various metal ions exchanged revealed that alkaline earth Y-type zeolites posses higher catalytic activity, while the zinc family, the alkali metals, and LaY-type zeolites possess lower activities [4,7].

The present study has been carried out in order to investigate the mechanism of disproportionation of NO by an infrared spectroscopic study.

★ Author for correspondence.
★★ Present address: Asahi Diamond Co., Kuju, Takatsu-ku, Kawasaki 213, Japan.

2. Experimental

2.1. MATERIALS AND REAGENTS

A Y-type zeolite in the sodium form (Union Carbide, SK-40) was ion-exchanged at 90 °C with a 10 wt% solution of ammonium nitrate. The resultant NH_4Y-type zeolite was further ion-exchanged with a 10 wt% solution of calcium nitrate and dried overnight at 110 °C. The composition of the $CaNH_4Y$-type zeolite thus prepared corresponds to $Ca_{24.9}(NH_4)_{6.2}Na(AlO_2)_{57}(SiO_2)_{135}\ nH_2O$ per unit cell. A chemical analysis was performed by flame and atomic absorption spectrophotometry. The $CaNH_4Y$-type zeolite of sample size 7–10 mg was pressed into thin plate of 20 mm∅, and the CaHY-type zeolite was prepared by removing NH_3 from $CaNH_4Y$-type zeolite, followed by the method described in the next procedure. NO, N_2O, and NO_2 gases were received from a commercial source (Takachiho Chemical Industry), and their purities were 99.6, 99.9, and 99.9%, respectively.

2.2. APPARATUS AND PROCEDURE

The measurement cell for the infrared spectrometer (Hitachi 295 type) was constructed of quartz, and was slightly modified according to the design used by Peri and Hannan [8]. The cell holding the sample was connected to a conventional vacuum line equipped with a mercury manometer and a gas storage vessel. The sample was treated at 150 °C for 3 h in a stream of dry CO_2-free air. Then the temperature of the sample was increased to 408 °C at a constant rate of 0.5 °C/min, where the sample was kept for 4 h, and then evacuated (10^{-6} Torr) for 2 h at the same temperature. After a series of these treatments, an adsorbed gas was introduced into the system at room temperature and all infrared spectra were recorded while the sample was at this temperature.

3. Results

3.1. INFRARED SPECTRA OF NO

Figure 1 shows the time-variation of infrared spectra produced when NO is adsorbed on CaHY-type zeolite: (1) the spectrum of CaHY-type zeolite itself after the degassing procedure at 408 °C (blank), (2) 100 Torr of NO was added to the system at 23 °C for 10 min, (3) maintained for 2 h, (4) maintained for 20 h (5) after degassing for 10 min at 23 °C, (6) after degassing for 1 h, (7) after degassing for 24 h, (8) 100 Torr of NO was added at 23 °C again for 10 min, (9) maintained for 48 h. These important results indicate that the spectra strength of the adsorbed species changed with the variation of the time of adsorption.

3.2. INFRARED SPECTRA OF N_2O

Figure 2 shows the change in the spectra produced when N_2O is adsorbed on CaHY-type zeolite: (1) blank, (2) 10 Torr of N_2O was added at 23 °C and maintained for 2 h, (3) after degassing for 10 min at 23 °C. The sharp peak at 2244 cm^{-1} in Figure 2 was assigned to adsorbed N_2O.

3.3. INFRARED SPECTRA OF NO_2

Figure 3 shows the spectra produced when NO_2 is added to CaHY-type zeolite: (1) blank, (2) 10 Torr of NO_2 was added at 23 °C for 10 min, (3) maintained for 2 h, (4) after degassing

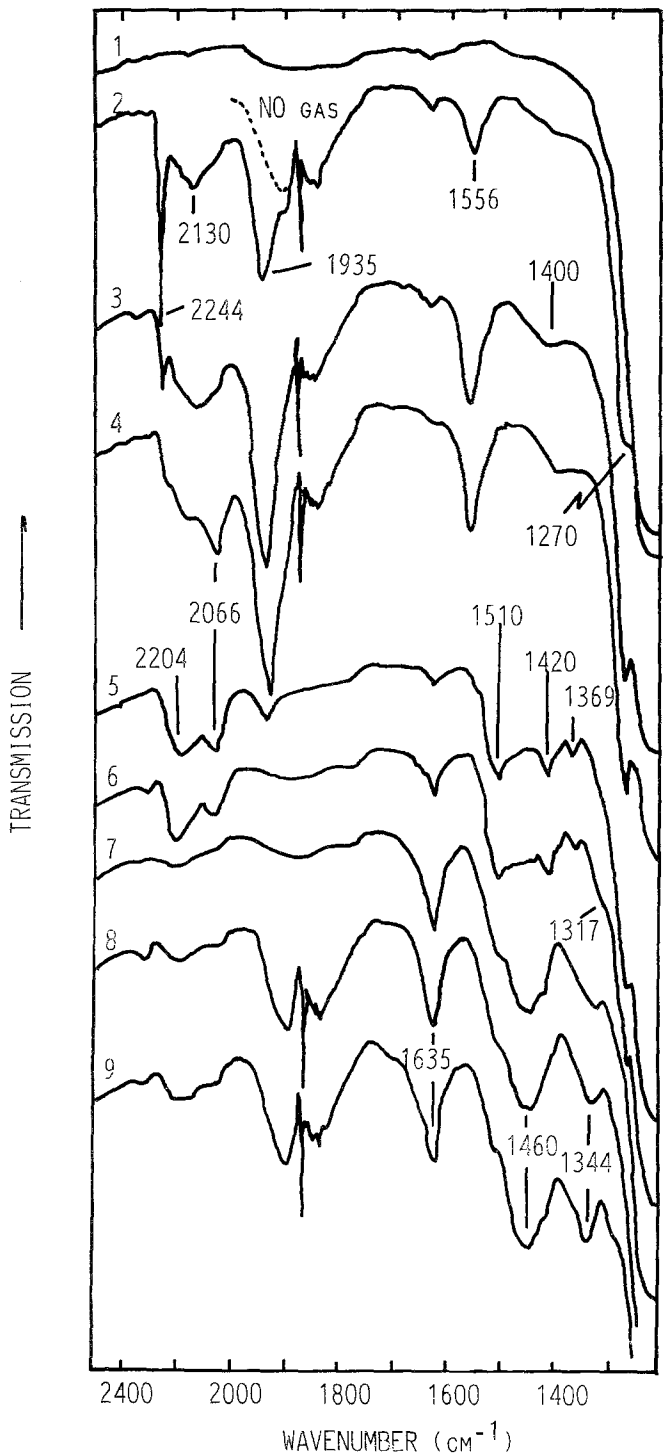

Fig. 1. Spectra produced when NO is adsorbed on CaHY zeolite: (1) degassed to 408°C, (2) 100 Torr of NO added at 23°C for 10 min, (3) maintained for 2 h, (4) maintained for 20 h, (5) degassed for 10 min at 23°C, (6) degassed for 1 h, (7) degassed for 24 h, (8) 100 Torr of NO added at 23°C again for 10 min, (9) maintained for 48 h.

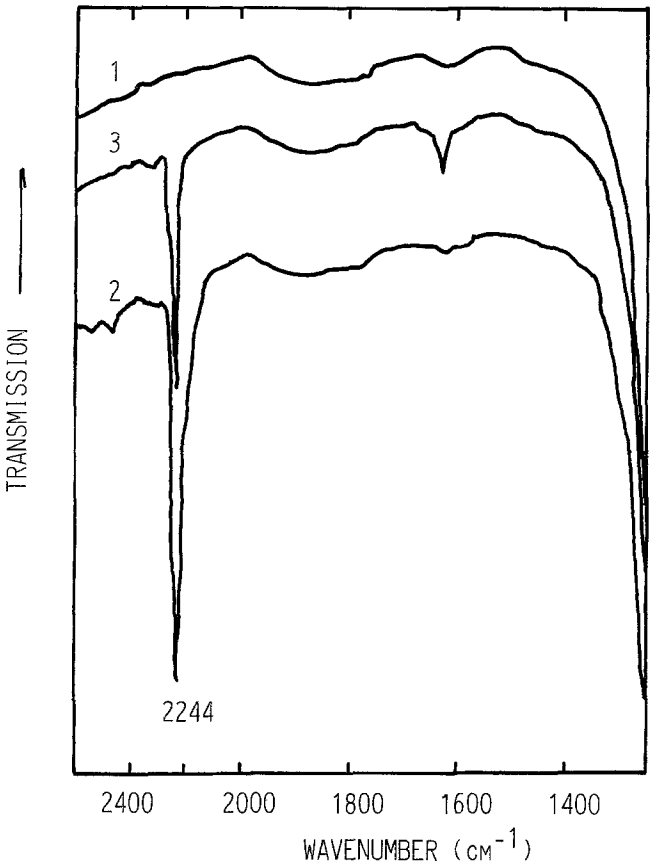

Fig. 2. Spectra produced when N_2O is added to CaHY zeolite: (1) degassed to 408 °C, (2) 10 Torr of N_2O added at 23 °C for 2 h, (3) degassed for 10 min at 23 °C.

for 10 min at 23 °C. In Figure 3 the peaks at 1750, 1635, and 1250 cm^{-1} disappeared or diminished upon the brief evacuation for 10 min. The peak at 1750 cm^{-1} can be assigned to physisorbed N_2O_4, and those at 1635 and 1250 cm^{-1} are assigned to physisorbed NO_2. The peaks at 2204, 1455, and 1344 cm^{-1} remained in spite of the evacuation for 10 min, and can be assigned to chemisorbed NO_2.

4. Discussion

4.1. IDENTIFICATION OF INFRARED ABSORPTION PEAKS INTRODUCED BY ADSORBING NO

Based on the infrared results, the peak assignments of spectra in Figure 1 can be made thusly. The peak at 2244 cm^{-1} is described as physisorbed N_2O. The absorption peaks at 2204, 1460, and 1344 cm^{-1} were produced when NO in the gas phase is evacuated, and are related to the adsorption of NO_2 on zeolite. Comparison with published data [9] enables us to clarify the assignments of spectra in Figure 1. In an infrared study of NO on CaY-type zeolite, which was obtained by evacuation at elevated temperatures, Chao and Lunsford assigned many kinds of infrared spectra to respective adsorbing species for NO [3]. Low and Yang reported the assignments for infrared spectra of NO adsorbed on CaO [10]. Table I, which is compiled

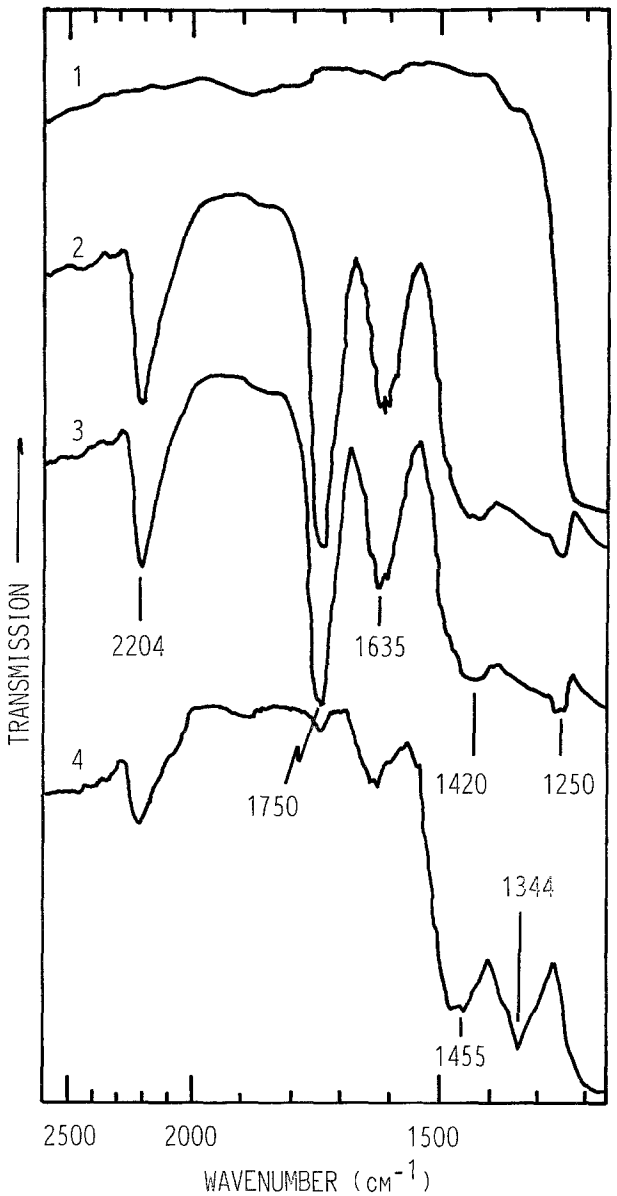

Fig. 3. Spectra produced when NO_2 is added to CaHY zeolite: (1) degassed to 408 °C, (2) 10 Torr of NO_2 added at 23 °C for 10 min, (3) maintained for 2 h, (4) degassed for 10 min at 23 °C.

from the literature, lists the assignments of infrared bands produced by the adsorption of NO. The peaks at 1935, 1556, and 1270 cm^{-1} change with time in the same manner and are regarded as arising from the same species, N_2O_3 [3]. Those at 2204 and 2066 cm^{-1} can be assigned to NO_2^+. The peaks at 1460 and 1344 cm^{-1} are assured to come from covalently bonded NO_3. The sharp peak at 1870 cm^{-1} is ascribed to physisorbed NO. With reference to curves (2), (3) and (4) in Figure 1, one can see that the peak at 2244 cm^{-1} appeared in the earlier stage of adsorption, and diminished gradually as the contact time increased. Since this peak can be ascribed to N_2O_3 we can consider that N_2O is formed by the dispropor-

Table I. Assignments of Infrared Spectra of NO_x

}(N_2O)	2250 cm^{-1}				*
Ca^{++}] $O_2N-N=O$	1935	1565	1305		
Ca^{+}]$--N_2O$	2040	2200			
}-ONO	1470				
NO^-	1000-1100				**
NO^+	2175	1600	1303		
NO_2	1365	1337			
NO_3^-	1365	1337			
COVALENT	1540	1510	1310	$Ca(O)_2N=O$	
NO_x	1458	1331	1281	$Ca-O-NO_2$	
NO	1876			GAS	***
$[NO]^+$	2220				
N_2O	2224	1286		GAS	
	2238	1293		SOLID	
NO_2	1612	1318		GAS	
	1624			SOLID	
$[NO_2^-]$	1335	1325		$K_2Ca[Ni(NO_2)_6]$	
	1396	1381	1332	$K_3[Co(NO_2)_6]$	
$-NO_2$	1582	1384		CH_3NO_2	
$[NO_2^+]$	2360	1400		CONC HNO_3	
	1685	1293		CL-NO_2(COVALENT)	
ONO	1468	1065		$[Co(NH_3)_5ONO]CL_2$	
	1640	1292	3426	HONO TRANS	
	1692	1260	3590	HONO CIS	
$[ONO]^-$	1335	1250			
N_2O_2	1862	1768		-190°C IN CO_2	
N_2O_3	1863	1589	1297		
N_2O_4	1712	1380			
NO_3^-	1400				

* Frequency of adsorbing NO on CaY zeolite, according to Chao et al. [3].
** Frequency of adsorbing NO on CaO, according to Low et al. [10].
*** According to Nakamoto [9].

tionation of NO as soon as NO molecules make contact with CaHY-type zeolite, and the N_2O molecules so formed desorb gradually with the passage of time. The peaks at 2130, 2066, and 2204 cm^{-1} are either NO^+ or NO_2^+. Since the 2130 cm^{-1} peak was strong in the earlier adsorption stage and reappeared upon evacuation, the peak may be assigned to NO^+. On the other hand, the 2066 and 2204 cm^{-1} peaks are assigned to NO_2^+ since the peak intensity

increased in the final stage of adsorption and remained even after evacuation. Since the 1400 cm^{-1} peak showed the same variation as the 2204 cm^{-1} peak, it was ascribed to either NO_2^- or NO_3^-. When NO gas was evacuated after maintaining 20 h, as shown in curve (5) in Figure 1, the absorption peaks of NO^+ and N_2O_3 diminished and new peaks appeared. Immediately upon evacuation, new absorption peaks appeared at 1510, 1420 and 1369 cm^{-1} besides NO^+. With further evacuation these peaks diminished and other new peaks appeared at 1344, 1400, and 1635 cm^{-1}. These are the same bands as those obtained by evacuation of adsorbed NO_2 on CaHY-type zeolite, as shown in Figure 3. These phenomena indicate that the chemisorbed NO_2 resulted from the gradual expulsion of NO from N_2O_3 on the zeolite surface. Though Chao and Lunsford reported the appearance of an absorption peak at 1470 cm^{-1} due to covalently bonded NO, the peak at 1510 cm^{-1} which appeared upon degassing was ascribed to ONO species. Since it is known that NO_3^- absorption peaks appear near 1400 cm^{-1}, the peaks at 1420 and 1369 cm^{-1} are attributed to NO_3^-. The peaks at 1635 and 1317 cm^{-1} vary in the same manner, and are assigned to NO_2 species. (NO_x compounds having absorption peaks in the region of 1600 to 1650 cm^{-1} are considered as either NO_2 or ONO; the ONO species has a strong vibrational frequency near 3300 cm^{-1}. However, we were unable to find such a band.) The intensity of the peaks at 1460 and 1344 cm^{-1} increased gradually with long evacuation time, and these two absorptions are ascribed to covalently-bonded NO_3, as pointed out by Low and Yang [10]. Curves (8) and (9) in Figure 1 are the spectra measured for readsorption after degassing. In spite of readsorption of NO, the peaks at 1935, 1566, and 1270 cm^{-1} ascribable to N_2O_3 species were not observed, while the physisorbed NO absorption peak appeared in the region of 1750 to 1870 cm^{-1} and a slight

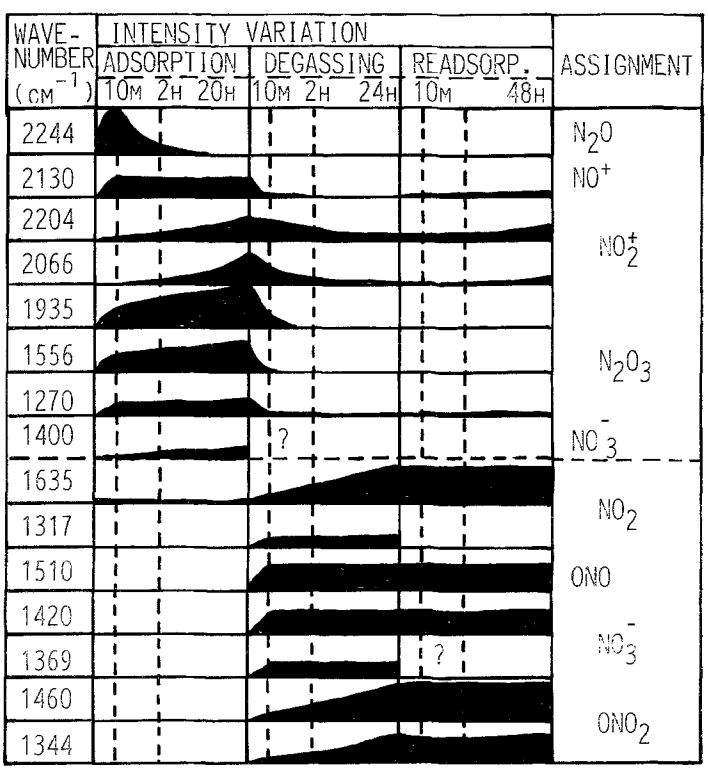

Fig. 4. Band relations of the spectra of Figure 1.

absorption peak of NO^+ was also noted. Therefore, we can state that N_2O_3 species were not formed by readsorption of NO without evacuation. However, it is clear that the readsorption of NO brings about absorption peaks due to N_2O_3 (formed by disproportionation with 10 min evacuation).

The absorption intensity of spectra from Figure 1 are rearranged in Figure 4 in order to help understand the mechanism for NO adsorption on CaHY-type zeolite. In Figure 4, it is easily seen that the major products of adsorption of NO on CaHY-type zeolite are N_2O and N_2O_3. Further, the amount of N_2O decreased with an increase of adsorption time. On the other hand, the NO_2^+ species increased gradually with the desorption of the N_2O. In the case of evacuation of NO, major adsorption species are NO_3^- and ONO in the earlier stages of evacuation, but after some time the main species became NO_2 and ONO_2.

4.2. MECHANISTIC MODEL

On the basis of the above discussion, a mechanistic model of the disproportionation reaction of NO on CaHY-type zeolite can be proposed (Figure 5). The model is explained as follows. In the first step, 1, NO molecules interact with a positively charged Ca^{2+} site at room

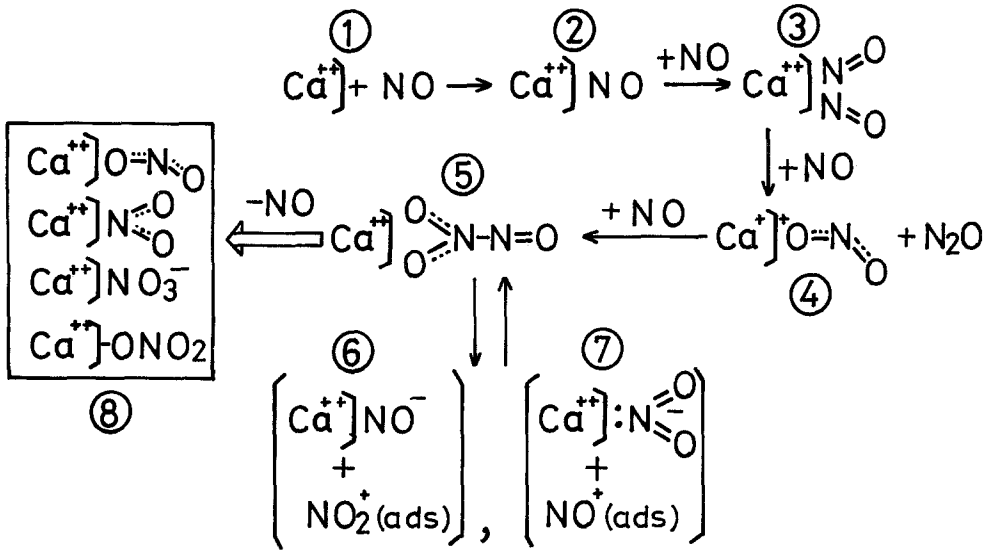

Fig. 5. Mechanistic model of disproportionation reaction of NO on CaHY zeolite.

temperature. Thus, NO molecules adsorb on the Ca^{2+} site in the second step, 2. In addition, this adsorbed species has been confirmed by an ESR study of adsorbed NO CaHY-type zeolite [11]. The chemisorbed NO species on the Ca^{2+} site interact with NO molecules in the gas phase, and the resulting adsorbed N_2O_2 dimers are stabilized on the zeolite surface in step 3. (Yet, it is not clear from the infrared studies whether an adsorbed N_2O_2 has more than a transient existence on CaHY-type zeolite.) The next step, 4, involves the interaction between an adsorbed N_2O_2 and a third NO molecule in the gas phase. N_2O and NO_2^+ are formed by rearrangement on the zeolite surface. The resulting N_2O was produced immediately in the earlier stage of adsorption and began to desorb into the gas phase gradually after 10 min.

The remaining NO_2^+ on CaHY-type zeolite in step 4 may interact with NO molecules in the gas phase, producing adsorbed N_2O_3 species. This is shown as step 5. Thus, the disproportionation reaction of NO ($4\,NO \rightarrow N_2O + N_2O_3$) has been completed. Furthermore, NO^+ and NO_2^- (step 7) and a very small amount of NO^- and NO_2^+ (step 6) were observed. It follows that an equilibrium involving steps 5, 6, and 7 is reached in the final part of the disproportionation reaction of NO on CaHY-type zeolite. On the other hand, removal of the gas phase NO led to the disappearence of N_2O_3 (step 5), and the production of ONO, NO_2, NO_3^- and ONO_2 (step 8).

From the facts described above, it is clear that one should pay attention to the adsorption of N_xO_y species in a discussion of the reactivity of NO on a zeolite.

References

1. W. E. Addison and R. M. Barrer: *J. Chem. Soc.* **70**, 757 (1955).
2. A. V. Alekseyev, V. N. Filimonov, and A. N. Terenin: *Dokl. Akad. Nauk. SSSR* **147**, 1392 (1962).
3. C. C. Chao and J. H. Lunsford: *J. Am. Chem. Soc.* **93**, 71 (1971).
4. Y. Kanno and H. Imai: *Mater. Res. Bull.* **17**, 1161 (1982).
5. Y. Kanno and H. Imai: *Nippon Kagaku Kaishi* 1559 (1982).
6. The nomenclature adopted in this paper is based on that used by Breck (D. W. Breck, *Zeolite Molecular Sieves*, John Wiley and Sons, New York (1974), p. 97). Site II is associated with the 6-membered ring of the sodalite cage, and is displaced towards the center of the super cage.
7. Y. Kanno and H. Imai: *Mater. Res. Bull.* **18**, 945 (1983).
8. J. B. Peri and R. B. Hannan: *J. Phys. Chem.* **64**, 1576 (1960).
9. N. Nakamoto, *Infrared and Raman Spectra of Inorganic and Coordination Compounds*, John Wiley & Sons, New York (1978).
10. M. J. D. Low and R. T. Yang: *J. Catal.* **34**, 479 (1974).
11. Y. Kanno and H. Imai: unpublished data.